JOURNAL OF CATALYSIS 85, 31–43 (1984)

Sulfur-Passivated Nickel Catalysts for Carbon-Free Steam Reforming of Methane

J. R. ROSTRUP-NIELSEN

Haldor Topsøe A/S, Nymøllevej 55, DK-2800 Lyngby, Denmark

Received October 25, 1982; revised June 21, 1983

It has been observed that carbon-free steam reforming of methane can be obtained on a partly sulfur-passivated nickel catalyst under conditions which, without the presence of sulfur, would result in formation of whisker carbon. This effect has been studied by means of kinetic experiments and thermogravimetry. The kinetic data can be explained by simple blockage of the surface as reflected in the observed kinetic orders and activation energy. The studies of carbon formation confirm a threshold coverage of about 70% of full coverage below which the inhibition of carbon is not effective. Above this coverage, amorphous carbon structures may be formed at very high carbon potentials. The retarding effect of sulfur on carbon formation is a dynamic phenomenon. Sulfur inhibits the rate of carbon formation more than the rate of the reforming reactions. The effects are explained by assuming that a large ensemble is involved in the nucleation of carbon, whereas the reforming reaction can proceed on the small ensembles left at high sulfur coverages.

INTRODUCTION

Steam reforming of natural gas is a well-established process (*1*) for the manufacture of synthesis gases and hydrogen. These applications involve operation with surplus steam to achieve the wanted equilibration of the reactions:

$$CH_4 + H_2O = CO + 3H_2 \quad (1)$$

$$CO + H_2O = CO_2 + H_2 \quad (2)$$

However, other applications aim at operation with minimum steam surplus, i.e., at O/C ratios close to 1, as for instance in the manufacture of reducing gas for direct reduction of iron ore (*2, 3*). Another trend has been the wish to operate at low H/C ratio to achieve the optimum CO/H_2 ratio for alcohol syntheses or oxosyntheses. This can be obtained by using carbon dioxide alone or mixed with steam as oxidant:

$$CO_2 + CH_4 = 2CO + 2H_2 \quad (3)$$

Reaction (3) has the advantage that it involves almost no condensation of product steam.

Operation at low O/C and H/C ratios involves the risk of carbon formation:

$$2CO = C + CO_2 \quad (4)$$

$$CH_4 = C + 2H_2 \quad (5)$$

The carbon grows as whiskers, normally with a nickel crystal at the top. It is generally believed (*4, 5*) that the mechanism involves diffusion of dissolved carbon in the nickel crystal.

Whether or not carbon is formed from methane is a result of a kinetic balance between the reversible reactions (1) to (5). Carbon will nucleate if the steady state activity (concentration) of carbon dissolved in the nickel crystal, a_c^s, exceeds the activity at saturation, a_c^L. Using the procedure of Williams *et al.* (*6*), the steady-state carbon activity can be expressed by (*1*):

$$a_c^s = \frac{a_c^{eq}}{1 + (k_g/k_c \cdot K_p(5)) \cdot K_w \cdot f(p_{H_2O}, p_{H_2})} \quad (6)$$

in which a_c^{eq} is the carbon activity at equilibrium with a given gas composition (not necessarily an equilibrated gas). In principle, a_c^{eq} should be referred to carbon dissolved in nickel:

$$a_c^{eq} = K_p(5) \cdot a_c^L \cdot \frac{p_{CH_4}}{p_{H_2}^2}. \quad (7)$$

0021-9517/84 $3.00

However, for simplicity, a_c^{eq} is referred to graphite in this paper (i.e., $a_c^L = 1$).

When the gas phase is equilibrated the denominator in Eq. (6) becomes equal to one, and carbon formation is then a question of whether the equilibrated gas shows $a_c^{eq} = K_p(5) \cdot (p_{CH_4}/p_{H_2}^2) > 1$ (i.e., $-\Delta G_e > 0$).

The thermodynamic calculations should take into consideration that $K_p(5)$ is affected by the deviation of the whisker structure from ideal graphite (*1, 7*).

This "principle of equilibrated gas" is usually applied to predict operational limits in steam reforming, thus disregarding the effect of the denominator of Eq. (6) in decreasing the carbon activity. The principle is justified, because the gas in the interior of the catalyst pellet at industrial conditions will be at equilibrium (*1*) ($\eta < 0.1$).

However, it was reported earlier (*8*) that in the presence of substantial quantities of sulfur, it was possible to operate without carbon formation under conditions for which the principle of equilibrated gas predicts carbon formation. Table 1 shows data (*8*) indicating the existence of a threshold content of hydrogen sulfide in the feed gas below which rapid carbon formation occurs.

TABLE 1

Optimum Sulfur Content for Sulfur-Passivated Reforming

Expt No.	1	2	3	4
S in feed, vol ppm H_2S	28	14	5	1
(H_2S/H_2) feed $\times 10^6$	90.9	45.5	16.2	3.2
θ_s[a] (feed gas) 850°C	0.91	0.87	0.83	0.75
θ_s[a] (equil. gas) 850°C	0.86	0.83	0.78	0.70
CH_4 (dry exit), vol%	0.71	0.70	0.36	—
Duration, h	47	42	95	5[b]
Carbon formation	No	No	No	Yes

Note. Integral flow reactor III. Catalyst A, 4 × 4-mm cylinders T_{inlet} = 520°C, T_{exit} = 945–948°C, P_{exit} = 0.3 MPa. Feed flows (mol/h): H_2O = 0.9, H_2 = 4, CO = CO_2 = CH_4 = 2.7, O/C = 1.11, H/C = 2.54 for Eq. (4): $-\Delta G_e > 0$ for $T > 840$°C, $-\Delta G_a$ (inlet) > 0 for $T < 677$°C. The catalyst was activated and sulfided overnight at increased steam/gas ratio. Sulfur was added as ammonia sulfide dissolved in water.

[a] Calculated by Eq. (8).

[b] Carbon formation was rapid and no gas analysis was taken.

Hydrogen sulfide chemisorbs on the nickel surface (*9, 10, 34*). The composition (*9*) of the saturation layer (44.5×10^{-9} g S/cm^2 Ni) does not vary significantly from face to face. It corresponds to approximately 0.5 sulfur atom per nickel atom on the (100) surface, in agreement with a $c(2 \times 2)$ structure (*9*). On the (111) surface, the structure is more complex (*11, 34*).

At complete coverage, the sulfur blocks the nickel surface which means that adsorbed carbon atoms cannot be dissolved into the nickel crystal (*7, 12*), and hence that the whisker growth mechanism is blocked. This effect is observed in various systems (*13–17*).

For the steam reforming reaction, a complete coverage of the nickel surface with sulfur results in total deactivation (*1, 18*). From the data in Table 1, it appears that above a certain sulfur coverage, there are still sites available for the reforming reaction whereas sites for carbon formation have been passivated.

The scope of this work was to study the reaction kinetics under these conditions as well as under the conditions for carbon formation.

EXPERIMENTAL

1. Apparatus and Catalysts

Three different reactor systems were used. Characteristic data are summarized in Table 2. These include a differential flow reactor (I) for kinetic and coking studies, a TGA unit (II) (*7, 13*) attached to a gas chromatograph (thus allowing simultaneous measurements of rates for reforming and coking reactions), and an integral flow reactor (III) for the simulation of industrial conditions.

The study included three different catalysts with properties as listed in Table 2. Catalyst A was taken from an industrial reducing gas plant after 1 year of operation.

TABLE 2

Summary of Reactor and Catalyst Data

Reactor	I	II	III
Type	Differential	TGA[a]	Integral
Tube diameter, mm (internal)	6	20	22.6
Cat. vol, cm^3	Approx 1	Single pellet	405
Cat. size, mm	0.3–0.5	4.5	3–5
Total feed, mol/h	1.12	1.12	Approx 13
Catalyst	**A**	**B**	**C**
Type	Ni/Al_2O_3	$Ni/MgAl_2O_4$	$Ni/MgAl_2O_4$
Ni, wt%	16.3	13.1	14.7
S content, wt ppm	20	<20	50
S capacity, s_0, wt ppm	200–400	360	—
Ni area, m^2/g	0.5–0.9	0.8	Est. 0.9
Density, g/cm^3	2.6	2.3	2.2
D_{eff} (CH_4, 0.1 MPa), m^2/h	0.03 (900°C)	0.10 (700°C)	0.03 (700°C)

[a] Unit described previously (*7, 13*).
[b] Chemisorption of H_2S at 500°C (*1*). Ni area = $s_0/440$ m^2/g.

This was done to have a stabilized catalyst, but it turned out that the sample had substantial variations in nickel surface area (see Table 2). Catalyst B was used as a 4.5 × 4.5-mm cylinder suspended in the wire of the TGA unit (II).

2. *Feed gas*

H_2 was supplied from an electrolyzer. Other gases were available in bottles. CH_4 contained impurities of less than 0.05% (mainly CO_2) with no higher hydrocarbons detectable by gas chromatographic analysis. In reactor II, H_2 and He were purified over copper. Other gases were used unpurified.

3. *Procedures and Evaluation*

Sulfur coverage. Experimental details are given with the presentation of results in Tables 1 and 3 and Figs. 2 to 6. Sulfur cov-

TABLE 3

Survey of Kinetic Studies: Dry Feed Gas

	Experiment No. and number of measurements					
	1030 10	1045 9	1025a 36	1025b 15	1037a 11	1037b 12
				Variation		
	CH_4[a]	CO_2	H_2S	H_2	Temp	Temp
Temp (°C)	900	900	900	900	850–924	851–930
Feed gas (vol %)						
H_2	25–35	ca. 14	ca. 25	8–41	ca. 27	ca. 66
CO_2	32–45	20–62	ca. 39	ca. 30	ca. 38	ca. 19
CH_4	20–44	ca. 25	ca. 36	ca. 25	ca. 35	ca. 15
H_2S (ppm)	10	10	5–30	10	10	10
Reforming (mol/g/h)						
$A_R \times 10^{-7}$[b]	3.11	2.10	1.75	1.07	3.00	2.60
SD $\times 10^{-7}$[c]	0.44	0.23	0.49	0.32	0.33	0.30
Reverse shift (mol/g/h)						
$A_S \times 10^{-5}$[b]	3.74	2.56	2.11	1.10	3.57	3.36
SD $\times 10^{-5}$[c]	1.06	0.82	0.67	0.31	0.85	0.52

Note. Fit of data to Eqs. (10) and (11). Reactor I: See Table 2. Catalyst A: Activation 2 h in H_2 at 800°C. Sulfidation >2h at $H_2S/H_2 = 250 \times 10^{-6}$, 10 liters (STP)/h. Stabilization approx 72 h at test conditions. Feed: Total 25 liters (STP)/h. One partial pressure varied randomly with N_2 as balance.

[a] No balance of N_2, constant flows of CO_2 and H_2.
[b] Partial pressures in MPa.
[c] Standard deviation for single measurements.

erages θ_s were calculated from

$$\theta_s = 1.45 - 9.53 \times 10^{-5} \cdot T + 4.17 \times 10^{-5} \cdot T \cdot \ln \frac{p_{H_2S}}{p_{H_2}} \quad (8)$$

(T in deg K).

This expression was found by Alstrup *et al.* (*10*) from a series of tests at temperatures and sulfur contents in the ranges applied in this study. As shown in Fig. 1, Eq. (8) can be approached by a simpler expression:

$$1 - \theta_s = 0.293 \exp(-4300/T) \left(\frac{p_{H_2S}}{p_{H_2}}\right)^{-0.3}. \quad (9)$$

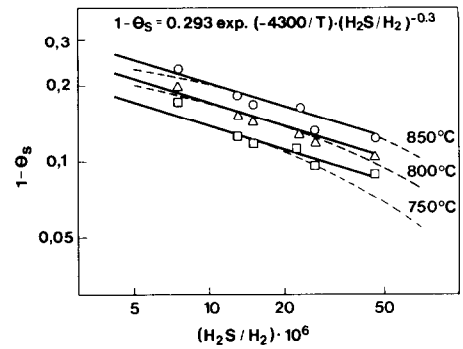

FIG. 1. Chemisorption of hydrogen sulfide on nickel. Measured data from Alstrup *et al.* (*10*). Plot of Eq. (9).

Transport restrictions. Calculations indicated negligible influence of mass and heat transfer on the measured rates in reactor I ($\eta > 0.9$).

The conditions in the TGA unit, reactor II, were more complex. The tests in the TGA unit involved difficulties in determining the temperature of the catalyst pellet because of the large heat of reaction in steam reforming. For this reason, a series of tests was carried out (in the absence of sulfur) with the pellet attached to a thin (0.1-mm) Pt–Rh thermocouple. The results, which confirmed the existence of a temperature drop of 35–40°C from the gas to the catalyst pellet, formed the basis for a formula correlating T_{cat} with the measured T_{gas} and T_w (see Table 3). This formula was used to correct temperatures in other TGA experiments.

Calculations showed that mass transport restrictions did not affect the measured rates in the TGA unit in the presence of sulfur ($\eta \sim 0.9$), but in the absence of sulfur the much higher reaction rates resulted in diffusion restrictions ($\eta \sim 0.5$).

RESULTS

1. Kinetics

The kinetic data from reactor I were evaluated by means of a computer program

TABLE 4

Experiments in CH_4/H_2 Mixtures

Expt No.	$\frac{H_2S}{H_2} \times 10^6$	θ_s	CH_4 (vol%)	$-\Delta G_e$ (kJ/mol)	Carbon structure[a]
6	0	0	4.0	0.9	None
8	0	0	4.5	1.2	Traces, whisker
7	0	0	4.8	1.3	Whisker
15	0	0	16.1	4.6	Whisker
14	0.5	0.66	16.5	4.7	Whisker + amorphous
12	1	0.70	4.8	1.3	Amorphous
13	1	0.70	16.4	4.6	Amorphous
10	27	0.85	5.4	1.6	Amorphous
11	27	0.85	17.9	4.9	Amorphous

Note. Reactor I, 0.4 g catalyst A, 850°C, 20 liters (STP) H_2/h. Activation: 1 h, 850°C; CH_4 added after 24 h in H_2S/H_2 as indicated, duration with CH_4: 16–20 h.

[a] From electron microscopy.

which performs a kinetic integration with specified kinetics for reactions (1) and (2). The data were fitted to kinetic expressions of power law form including a term for H_2S. Trends in the calculated rate constant were checked by regression analysis, and the kinetic parameters were adjusted to minimize the variance.

For experiments in dry atmosphere, this procedure assumes that the rate of the reverse shift reaction is significantly higher than that of the reforming reaction, in order to provide sufficient steam. This assumption is justified by the results of Bodrov and Apelbaum (*19*).

Dry feed gas. The results from the kinetic tests in dry feed gas are summarized in Table 3. The data show a reasonable fit to the rate expression for the reforming reaction (1):

$$r_R = A_R \exp(-32.1 \times 10^3/T) p_{CH_4}{}^{0.8} \cdot p_{H_2}{}^{0.3} p_{H_2S}{}^{-0.9}(1 - \beta) \quad (10)$$

whereas the fit to the reverse shift reaction (reverse (2)) is less accurate:

$$r_s = A_s \exp(-22.9 \times 10^3/T) p_{CO_2} \cdot p_{H_2}{}^{0.6} \cdot p_{H_2S}{}^{-0.7}(1 - \beta). \quad (11)$$

This uncertainty is probably due to the influence of the shift reaction in the gas phase and on hot walls, which may become significant at temperatures above 800°C (*20*). The scatter in A_R and A_S between different experiments can be ascribed to substantial variations within the catalyst sample as explained above (see Table 2). The term r_S is much larger than r_R ($k_S/k_R \sim 30$ at 900°C) which supports the assumption that the two reactions can be treated independently in the kinetic analysis.

The high activation energy and the negative reaction order with respect to hydrogen sulfide as well as the positive order with respect to hydrogen are noted for both reactions. The activation energy was not influenced significantly by the H/C ratio. Regression analysis for all tests results in E_R = 267 kJ/mol.

Wet feed gas. The experiments carried out in the presence of steam resulted in E_R = 227 kJ/mol as shown in Fig. 2. When the addition of steam was varied, the reaction rate was found to be zero order with respect to steam. Further, when carbon dioxide replaced steam at 900°C the rate constant was not affected.

Without sulfur. A single experiment was carried out in the presence of steam, but without the presence of sulfur. This showed a lower activation energy, E_R = 110 kJ/mol, which is in accordance with the values usually reported (*1*) for steam reforming of methane. The temperature variation of the specific rate is plotted in Fig. 2. The experiments were restricted to temperatures below those used in the presence of sulfur, because the sulfur-free test would be significantly influenced by diffusion restrictions at the high temperatures.

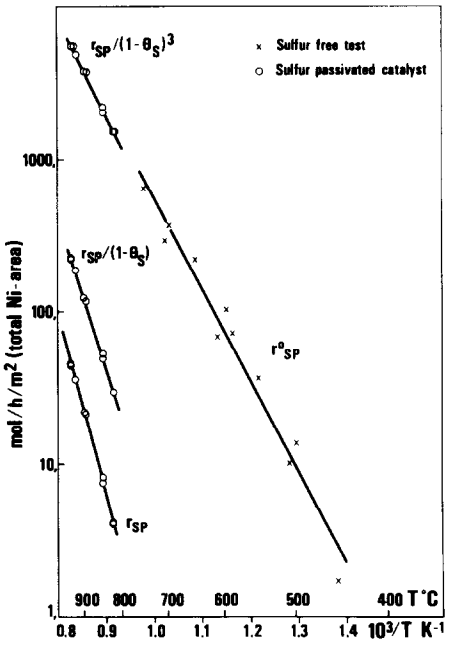

FIG. 2. Specific activity and sulfur passivation. Reactor I, catalyst A. Specific activity, r_{sp}, in tests with presence of sulfur. r_{sp} is referred to total nickel area. $r_{sp}{}^0$, specific activity under sulfur-free conditions. θ_s is calculated by means of Eq. (8). Experiment with sulfur passivation: H_2O/CH_4 = 1.0, H_2O/H_2 = 5.0, H_2S/H_2 = 2.8×10^{-5}, 0.1 MPa. Experiment under sulfur-free conditions: H_2O/CH_4 = 0.94, H_2O/H_2 = 2.5, 0.1 MPa.

TGA unit. The activation energy for the methane reforming reaction was also determined in the TGA unit in the presence of sulfur ($H_2S/H_2 = 9 \times 10^{-6}$) in the temperature range 750–830°C (see Fig. 3). The result, $E = 229$ kJ/mol, is close to that obtained in reactor I (see Fig. 2). This strongly supports the assumption that the TGA tests carried out in the presence of sulfur are not influenced by diffusion restrictions.

2. Carbon Formation

Experiments in CH_4/H_2 mixtures. A series of tests was carried out in reactor I at 850°C in mixtures of methane and hydrogen, which is a situation with no competition from gasification of the absorbed carbon. The denominator in Eq. (6) is unity and $a_c^s = a_c^{eq}$.

A number of experiments in sulfur-free feed were used to determine the methane content above which carbon was formed. The data in Table 4 show that this occurred at $-\Delta G_e = 1.2$ kJ/mol. This value corresponds to the deviation from graphite data to be expected for whisker carbon (*7*). Examination under an electron microscope confirmed the formation of the usual whisker-like carbon with nickel crystals at the top.

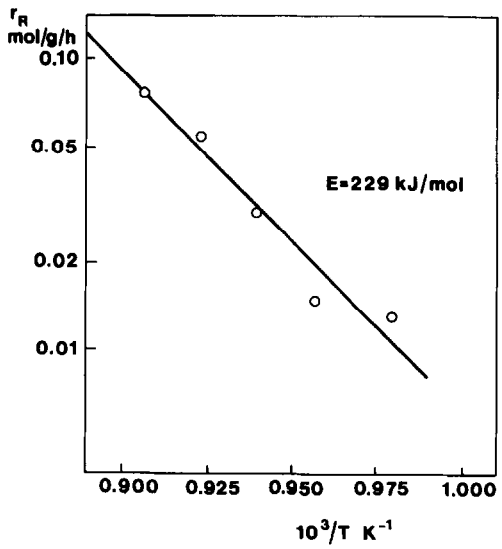

FIG. 3. Reforming rates in TGA unit. Reactor II, catalyst B. Feed (25 liters (STP)/h), vol%: H_2, 32; H_2O, 8; CH_4, 27; He, 33; $H_2S/H_2 = 2 \times 10^{-6}$. T_{cat} corrected as indicated in Table 5.

Experiments in the presence of sulfur ($H_2S/H_2 = 0.5$ to 27×10^{-6}) showed carbon formation close to the equilibrium point (see Table 4). Electron microscopy revealed a few normal carbon whiskers at $H_2S/H_2: 0.5 \times 10^{-6}$ ($\theta_s = 0.66$), but at higher sulfur coverages the carbon structure was amorphous with no usual whiskers. The amorphous carbon was in plate-like shapes as well as less-developed carbon whiskers, some with a number of threads from each nickel crystal ("octopus carbon" (*21*)).

In conclusion, a partial sulfur coverage was not able to inhibit carbon formation from a gas at gas phase equilibrium. However, above a coverage, $\theta_s \sim 0.7$, the usual whisker structure was replaced by more amorphous structures.

Reforming conditions, sulfur-free atmosphere. Results from experiments in the TGA unit (reactor II) in sulfur-free atmosphere are shown in Table 5. The critical ratio $(H_2O/CH_4)_{crit}$ indicating the onset of carbon formation was determined by interpolation of carbon formation and removal rates measured at different ratios of H_2O/CH_4.

The calculated carbon potentials $-\Delta G_e$ on the basis of the equilibrated gas at $(H_2O/CH_4)_{crit}$ result in values of $-\Delta G_e$ less than about 2 kJ/mol (except for one measurement) as in the CH_4/H_2 tests (Table 4). Again, this can be ascribed to the effect of the whisker structure (*7*). The results were similar when carbon dioxide replaced steam. The values of $-\Delta G_a$ calculated from the exit gas analyses were 20 to 40 kJ/mol. Hence, the data in Table 5 are in accordance with the "principle of equilibrated gas."

The result is not surprising in view of the low effectiveness factor ($\eta < 0.5$). Most of the catalyst is filled with gas close to equilibrium.

Reforming conditions with sulfur. The rates of carbon formation and steam re-

TABLE 5

Carbon Formation and Equilibrated Gas[a]

T_{gas} (°C)	650	750	850	750
T_{cat}[b] (°C)	613	704	812	662
H_2O/CH_4 (crit.)	1.2	1.1	0.88	1.75[c]
$p_{H_2}^2/p_{CH_4}$ actual gas = Q_a (MPa)	0.0034	0.0055	0.0161	0.0438
$p_{H_2}^2/p_{CH_4}$ equil. gas = Q_e (MPa)	0.221	0.722	1.099	0.306
K_p graphite data (MPa)	0.2660	0.819	2.468	0.4939
$-\Delta G_e^0 = RT \ln(K_p/Q_e)$ (kJ/mol)	1.6	0.9	(7.3)	2.3

[a] Sulfur-free feed gas, TGA unit (reactor II), catalyst B.

[b] The catalyst temperature was calculated from $a \cdot T_{cat}^4 + b \cdot T_{cat} = a \cdot T_w^4 + b \cdot T_{gas} - Q$. T in °C, Q (kJ/mol) is heat absorbed by the reaction; $a = 1.36 \times 10^{-11}$, $b = 5.04 \times 10^{-2}$; a and b fitted from experiments with pellet attached to thermocouple.

[c] CO_2/CH_4.

forming were measured simultaneously in the TGA unit (reactor II) in a series of tests with different sulfur contents in the feed. Results are shown in Fig. 4. Reaction rates are low and, as outlined above, the conditions can be considered without influence of mass transport restrictions. Sulfur inhibits the rate of carbon formation, r_c, more than the rate of the reforming reaction, $r_R \cdot r_c$, and r_R increase with $(1 - \theta_s)$ with the powers of 6.3 and 2.7, respectively. The power value for r_R is close to that shown in Fig. 2.

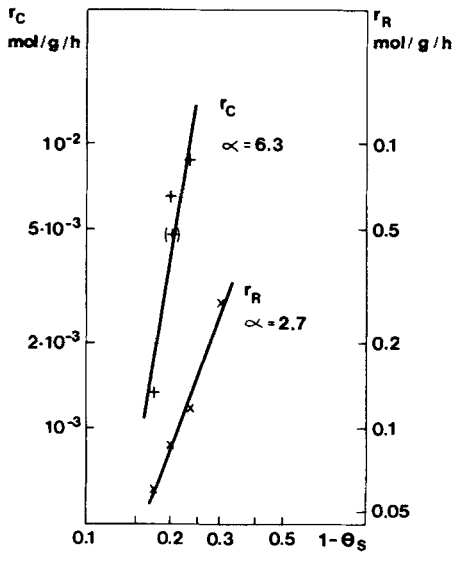

FIG. 4. Impact of sulfur on rates of carbon formation and steam reforming. TGA unit (reactor II). Catalyst B. Feed gas (total 30 liters (STP)/h), vol%: H_2, 27; He, 5; H_2O, 7; CH_4, 61. T_{gas} = 850°C. T_{cat} corrected (Table 5) and rates referred to 830°C, using E_R = 229 kJ/mol and E_c = 126 kJ/mol (5).

The carbon activities, a_c^{eq}, required for onset of carbon formation were determined in the TGA unit at different sulfur contents in feed. The methane flow was increased until onset of carbon formation and then decreased to onset of carbon gasification. The critical steam to carbon ratio was determined by interpolation. The carbon activity, a_c^{eq}, at equilibrium with the actual gas composition at $(H_2O/CH_4)_{crit}$ was calculated by Eq. (7) setting $a_C^L = 1$ for simplicity. This value corresponds to the condition for which the steady state activity a_c^s is equal to unity (i.e., onset of carbon formation).

Data are shown in Table 6 and Fig. 5. Additional tests were carried out in reactor I to determine $(H_2O/CH_4)_{crit}$ by trial and error. Results are shown in Table 6.

The graph in Fig. 5 illustrates how sulfur inhibits the nucleation of carbon. The carbon potential a_c^{eq} for onset of carbon formation decreases with the square of the free surface $(1 - \theta_s)$. This means that a_c^s increases with $(1 - \theta_s)^2$. The graph is semi-

TABLE 6

Steam Reforming on Sulfur-Passivated Catalysts: Carbon Activities for Onset of Carbon Formation

Expt No.	Oxidant	T_{gas} (°C)	T_{cat} (°C)	$\frac{H_2S}{H_2} \times 10^6$	Average inlet/exit θ_s[a]	O/C	H/C	H_2O/H_2	p_{H_2} (Mpa)	a_c^{eq}	a_c^{s}[b]	$-\Delta G_e$ (kJ/mol)
					Reactor I							
1039	CO_2	900	900	43	0.85	0.80	3.10	0.09	0.033	190	1.14	30
1045	CO_2		900	19	0.81	0.52	5.13	0.03	0.054	56	1.07	30
1089	H_2O		900	20	0.81	0.18	4.45	0.21	0.039	367	1.22	47
					Reactor II							
678	H_2O	850	838	13	0.82	0.20	6.0	0.20	0.027	145	0.79	35
677			837	7	0.80	0.22	6.2	0.20	0.027	105	0.76	34
676			829	6	0.79	0.22	6.2	0.18	0.028	102	0.88	33
679			832	3	0.76	0.24	6.4	0.19	0.026	77	0.90	32
(682)[c]			800	0.5	0.70	>0.22			—	—		
681		800	789	5	0.81	0.13	5.3	0.21	0.029	127	1.09	33
680			781	2	0.77	0.14	5.4	0.19	0.031	97	1.24	31
683			783	1.7	0.76	0.20	6.0	0.20	0.030	79	1.05	28
684			782	1.2	0.75	0.22	6.2	0.20	0.026	71	1.11	28

Note. Reactor I: Catalyst A, feed (25 liters (STP)/h): H_2, CH_4, CO_2 (or H_2O). Conversions approx 10%. Reactor II: Catalyst B, feed (25 liters (STP)/h) (Total flow liters/(STP)/h): Exp. No. 681, 27; Exp. No. 682, 26). H_2: 32%, H_2O: 8%, He + CH_4: 60%. Conversions 1–3%, T_{cat} corrected as in Table 5.

[a] Calculated from Eq. (8).

[b] $a_c^s = \dfrac{a_c^{eq}(1-\theta_s)^2}{6.17 \times 10^4 \cdot \exp(-7760/T) \cdot (H_2O/H_2) \cdot \sqrt{p_{H_2}}}$, $a_c^s = 1$ for onset of carbon formation.

[c] Rapid carbon formation at $H_2O/CH_4 = 0.22$, breakdown of catalyst.

quantitative only, because the temperature varied, but apparently the influence of temperature was minimum. The tests in reactor II were carried out at higher temperature and with different gas compositions and catalyst.

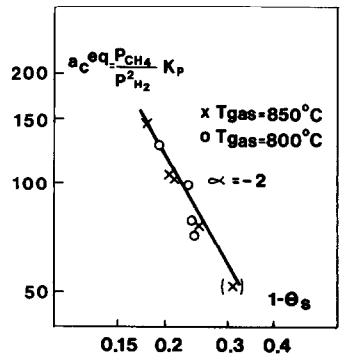

FIG. 5. Carbon activities at onset of carbon formation. TGA unit (reactor II). Catalyst B. Feed gas (total 25 liters (STP)/h), vol%: H_2, 32; H_2O, 8; He + CH_4, 60. Carbon activities calculated at $(H_2O/CH_4)_{crit}$ at various contents of sulfur in feed (Table 6). T_{cat} corrected as in Table 5. (×) Data for rapid carbon formation resulting in breakdown of catalyst pellet.

Attempts were made to correlate the data obtained in reactor I and II by fitting an expression for a_c^s in the form of Eq. (6). Results are shown in Table 6. It is evident that more experiments are required to allow formulation of a better model. Further, the potential for carbon in the equilibrated gas was calculated. Table 6 shows that the experiments were performed at $-\Delta G_e$ from 25 to 50 kJ/mol, i.e., at much larger values than reported in Table 5 for sulfur-free conditions.

Integral conditions. The test series described in Table 1 showed that carbon-free operation can be achieved above a certain sulfur coverage under ($\theta_s > 0.8$) conditions with potential for carbon formation. The equilibrated gas showed potential for carbon below 840°C (graphite data), i.e., in the heating-up zone of the reactor.

Another series was carried out at $H_2O/$

CH_4 = 0.7 under the conditions listed in Fig. 6. This corresponds to $-\Delta G_e$ increasing from 1.3 kJ/mol at the inlet to approx 6 kJ/mol at the exit, i.e., much lower values than indicated for onset of carbon formation in Table 6. Nevertheless, carbon was formed above approx 850°C and approx 750°C with 4 and 10 ppm H_2S in the exit gas, respectively. The carbon was formed at first in the interior of the pellets, as shown in Fig. 6. The sulfur coverages (on the basis of the equilibrated gases) in the carbon-forming zone were estimated to be 0.8–0.85. Sulfur analyses of the spent catalyst indicated no significant differences between the carbon-free shell (300 wt ppm) and the core (280 wt ppm when corrected for a carbon content of 21%). Electron microscopy showed formation of carbon whiskers of nonregular type.

DISCUSSION

Kinetics

The impact of sulfur on the reforming kinetics is significant. The large increase in activation energy might be explained by electron ligand effects (*22, 23*). Kiskinova and Goodman (*23*) concluded that the electronegativity factor plays a major role in explaining the poisoning of nickel by sulfur. At low coverages, on a (100) surface, sulfur occupies a fourfold hollow site independent of coverage and Kiskinova and Goodman (*23, 24*) found the methanation activity to decrease with $(1-4 \cdot \theta_1)$ indicating that each sulfur atom may quench the four neighboring nickel atoms. Similar results were reported by Erley and Wagner (*25*) who found that the dissociation of carbon monoxide on a (111) surface decreased with $(1-3 \cdot \theta_1)$.

However, at the high coverages of this study, the surface probably consists of islands of free nickel atoms surrounded by the saturation layer of approx 0.5 sulfur atom per nickel atom ($c(2 \times 2)$ structure on (100) surface) (*1, 10*) and hence the electron ligand effect is reduced.

The results on reforming kinetics may be explained in terms of physical blockage by chemisorbed sulfur. The increase of the activation energy can be ascribed to superposition of the chemisorption equilibrium.

For a reaction requiring an ensemble of m nickel atoms, the rate on the partly poisoned catalyst can be expressed by (13)

$$r_{sp} = r_{sp}^0(1 - a \cdot b\ \theta_s)^m \qquad (12)$$

in which θ_s is the sulfur coverage relative to saturation. The parameter a is the number of sulfur atoms per nickel atom at surface saturation, and it is close to 0.5, corresponding to the $c(2 \times 2)$ structure. Parameter b expresses the number of nickel atoms quenched per sulfur atom and is expected to be a function of coverage. Parameter b is assumed to be close to 2.0 (i.e., $a \cdot b = 1$ in the range considered here), since no nickel atoms are active at full coverage ($\theta_s = 1$) (*18*).

The specific rates referred to total nickel surface have been compared in Fig. 2 for data obtained on the sulfur-passivated catalyst and the sulfur-free catalyst, respectively. Low rates, r_R, on the sulfur-passivated catalysts are apparent. However, if rates are corrected according to Eq. (12), r_{sp}^0 shows reasonable agreement with the data on sulfur-free catalyst extrapolated to higher temperature. The agreement is obtained for $m = 3$:

$$r_{sp}^0 = r_{sp}/(1 - \theta_s)^3 \qquad (13)$$

which according to Eq. (12) should reflect that an ensemble of three nickel atoms is involved in the reforming reaction. The activation energy of r_{sp}^0 is estimated at 120 kJ/mol, being close to that obtained in the sulfur-free test (110 kJ/mol).

The rate of the sulfur-free catalyst can be expressed by (*1, 19*):

$$r_{sp}^0 = k^0 \exp(-13 \times 10^3/T) p_{CH_4} \cdot p_{H_2}^{\alpha} \qquad (14)$$

in which α may vary. Bodrov *et al.* (*35*) found α to vary from -1 to 0 with increasing temperature.

If so, the rate on the sulfur-passivated catalyst can be expressed by a combination

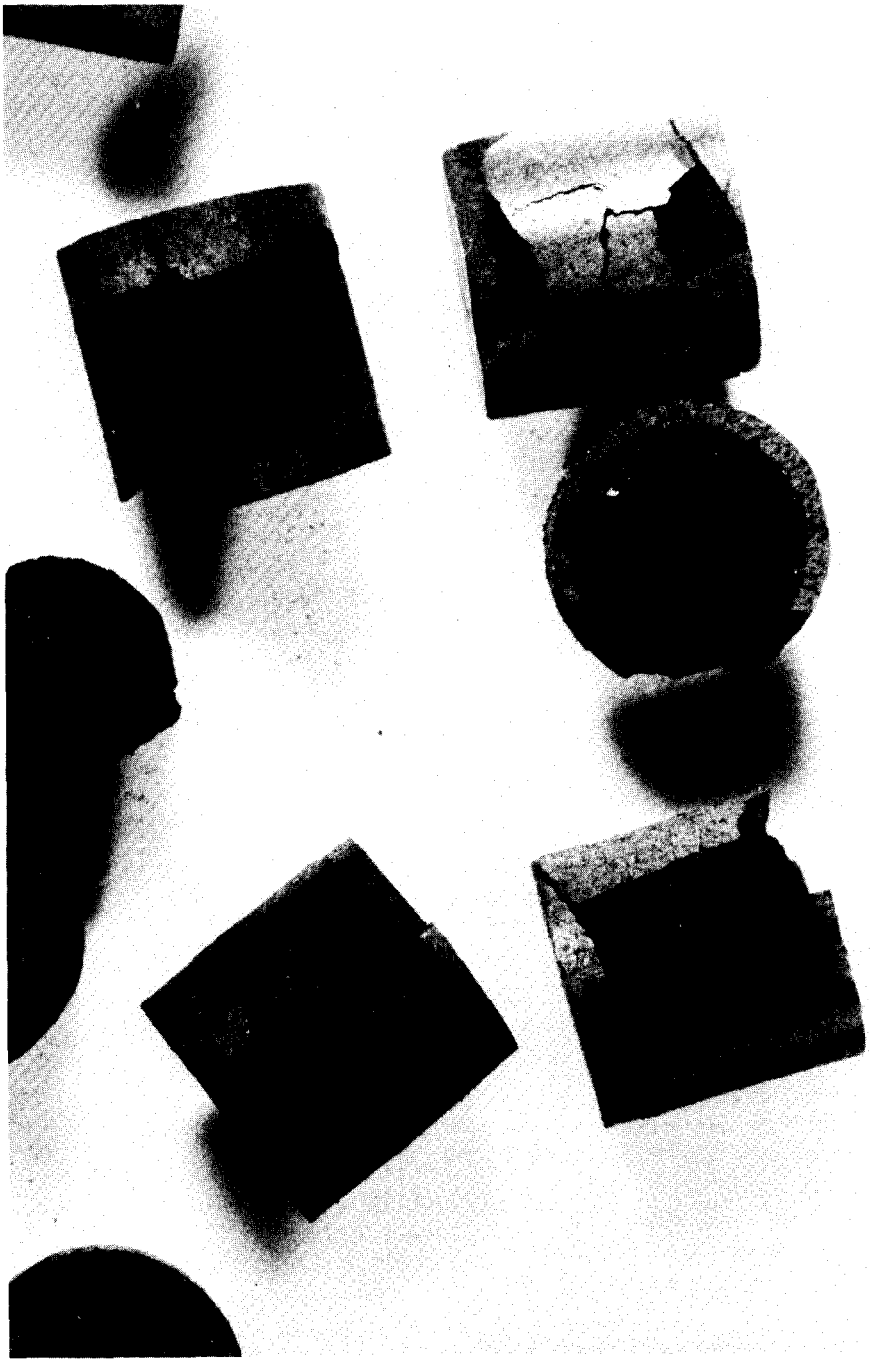

FIG. 6. Carbon formation on sulfur-passivated catalyst under integral conditions. Reactor III. Catalyst C. $H_2O/CH_4 = 0.7$, H_2O/H_2 (inlet) = 30, H_2S (inlet) = 7 vol ppm. T_{inlet}/T_{exit} = 515°C/905°C, P_{exit} = 0.3 MPa, SV_{cl} = 770 vol CH_4/vol cat/h. Duration 12 h. The exit gas was close to equilibrium of reactions (1) and (2). Carbon was formed at approx 750°C. With H_2S (inlet) = 18 vol ppm, carbon was formed at approx 850°C.

of (9) and (14):

$$r_{sp} = r_{sp}^{0}(1 - \theta_s)^3 = k \exp(-26 \times 10^3/T) p_{CH_4} \cdot p_{H_2}^{\alpha+0.9} \cdot p_{H_2S}^{-0.9}. \quad (15)$$

The activation energy, 217 kJ/mol, corresponds to the value found in the experiment, 227 kJ/mol. Equation (15) may also explain the experimental reaction orders with respect to hydrogen sulfide and hydrogen (Eq. (10)), whereas the reaction order with respect to methane differs.

Carbon Formation

Sulfur retards the rate of carbon formation more than the reforming rate (Fig. 4). Carbon is nucleated when the catalyst is at equilibrium with the gas phase and when the gas phase shows potential for carbon formation ($a_c^{eq} > 1$, $-\Delta G_a = -\Delta G_e > 0$). However, under conditions far from gas phase equilibrium the gasification of adsorbed carbon atoms results in a depression of the carbon activity and carbon-free operation can be achieved ($a_c^s < 1$), in spite of $a_c^{eq} > 1$ ($-\Delta G_a > 0$). This can be obtained also in situations where $-\Delta G_e > 0$ (Table 6).

The steady-state activity, a_c^s, depends on sulfur coverage (proportional to $(1 - \theta_s)^2$). The impact of sulfur coverage on nucleation of carbon is also reflected by the morphology of carbon. Above a certain coverage ($\theta_s \sim 0.7$–0.8), whisker carbon is not formed. This threshold value corresponds to observations by Erley and Wagner (*25*). Sulfur completely eliminated the dissociative adsorption of carbon monoxide into adsorbed carbon atoms at a coverage $\theta_1 = 0.33$ which is equivalent to $\theta_s \sim 2 \times 0.33 = 0.7$.

Under integral conditions, the situation becomes complex. In the test series reported in Table 1, the gas is far from equilibrium in the heating-up zone because of nearly complete sulfur coverage. When the reaction starts and the interior parts of the pellets are filled with equilibrated gas, the gas has no longer potential for carbon formation. Below a certain sulfur content in the feed (approx 1 ppm H_2S), the reforming reaction rate becomes significant below the carbon limit temperature, and carbon results because there is no depression of a_c^{eq} in the equilibrated gas.

In the test series described in Fig. 6, the carbon potential ($-\Delta G_e$) increases throughout the bed. This means that carbon is formed when the gas approaches equilibrium. This is illustrated in Fig. 6, where by accident the effectiveness factor is still so high that a steady-state situation prevails in the shell resulting in $a_c^s < 1$.

Ensembles

The increased selectivity for steam reforming at higher sulfur coverages may indicate that the ensembles of free nickel atoms available for the conversion of adsorbed methane are sufficient for the conversion with steam, but they are too small to allow the normal dissolution–precipitation nucleation (*4, 5*) of the carbon whisker. This means that $m' > n$ and m in

$$CH_4 \rightarrow CH_x\text{-}*_n \rightarrow C\text{-}*_m \rightarrow C\text{-}*'_m \rightarrow Ni,C \rightarrow C\text{-whisker}. \quad (16)$$

There is some evidence (*1, 26, 27*) that the reaction intermediate in steam reforming at sulfur-free conditions is adsorbed carbon atoms, $C\text{-}*_m$, rather than $CH_x\text{-}*_n$. This does not mean that the complete dissociation is necessary for steam reforming on a sulfur-passivated catalyst. $CH_x\text{-}*_n$ might well be the intermediate, if the complete dissociation is retarded by high sulfur coverage. On the other hand, studies by Chahar and Hightower (*28*) showed that the reactive species in methane–deuterium exchange on catalyst B was not influenced by the presence of sulfur which may indicate that $C\text{-}*_m$ is the intermediate for reforming. However, the result of Chahar and Hightower might reflect the exchange reaction on the nonpoisoned core of the catalyst particle.

The data in this study in any case indicate that the site, $*'_m$, required for dissolution of surface carbon into the bulk is larger than that required by the reforming reaction, whether this is CH_x-$*_n$ or C-$*_m$. It is easy to visualize that the movement of carbon atoms into the bulk nickel may well require a larger ensemble ($*'_m$) than does the (complete) dissociation of methane.

The idea of a large ensemble for nucleation of carbon is supported by the considerable inhibiting effect of hydrogen on carbon formation on nickel observed in mixtures of methane (*1*) or other hydrocarbons (*29*) in hydrogen.

It is evident that the concentration of the large ensembles for carbon nucleation will decrease drastically with sulfur coverage, but complex statistical calculations are required to quantify the effects, because the buildup of the saturation layer does not follow a random model (*30*). The process involves formation of islands of surface sulfide (*9*) which may become mobile (*31*) at the high temperatures of this study.

The control of exposed ensembles by means of sulfur resembles the effects studied in alloy catalysis (*32, 33*).

CONCLUSIONS

Sulfur retards the rate of carbon formation more than the rate of steam reforming. The effect can be explained by a blockage of the sites (ensembles). Apparently, the ensembles required for nucleation of carbon are larger than those for steam reforming. Above a certain sulfur coverage (θ_s = 0.7–0.8) the formation of normal whisker carbon is eliminated, but still formation of amorphous carbon is possible.

Under conditions far from gas phase equilibrium, the ensemble effect results in a reduction of the steady-state activity of carbon, thus allowing operation under conditions where a sulfur-free catalyst would show rapid carbon formation. This effect is a dynamic phenomenon. It vanishes when the gas phase approaches equilibrium.

ACKNOWLEDGMENTS

Thanks are given to Ms. Ulla Ebert Petersen and Mr. Niels Blom for assistance in performing the experiments and to Mr. Ib Alstrup, Dr. Carlos Bernardo, and Dr. Flemming Topsøe for stimulating discussions.

APPENDIX: NOMENCLATURE

A_R, A_s	preexponential factor for reforming and reverse shift reactions
D_{eff}	effective diffusion coefficient
E	activation energy
$-\Delta G_a$	affinity for Reaction (5), $-\Delta G_a = RT \ln(K_p(5)/Q_a) = RT \ln(K_p(5) \cdot p_{CH_4}/P_{H_2}^2)$
$-\Delta G_e$	affinity for Reaction (5) after equilibration of (1) and (2), $-\Delta G_e = RT \cdot \ln(K_p(5)/Q_e)$
K_p	equilibrium constant (standard state 298 K, 0.1 MPa)
K_w	adsorption constant for steam on catalyst
Q	heat absorbed by reaction
Q_a	reaction quotient in actual gas
Q_e	reaction quotient in equilibrated gas
T	temperature
T_{cat}	catalyst temperature
T_{gas}	gas temperature
T_w	external tube wall temperature
a, b	constants
a_c^s	steady-state activity of carbon, Eq. (6)
a_c^{eq}	carbon activity (Eq. (5)) at equilibrium with given gas composition
a_C^L	carbon activity at saturation of the nickel crystal, Eq. (7)
k_c	rate constant for dissolution of surface carbon in nickel
k_g	rate constant for gasification of surface carbon
k_R, k_S	rate constants per unit catalyst weight for reforming and reverse shift reactions $k = A \exp(-E/RT)$
m, n	numbers
r_c	rate of carbon formation per unit catalyst weight
r_R, r_S	reaction rate per unit catalyst weight for reforming and reverse shift reactions

r_{sp}^0 specific rate for sulfur-free catalyst
r_{sp} specific rate of poisoned catalyst referred to total nickel surface area
SD standard deviation
α kinetic coefficient
β Q_a/K_p
η effectiveness factor
θ_1 sulfur coverage expressed as sulfur atoms per nickel surface atom
θ_s sulfur coverage expressed as fraction of saturation

REFERENCES

1. Rostrup-Nielsen, J. R., *in* "Catalysis, Science and Technology" (J. R. Anderson and M. Boudart, Eds.), Vol. 5, Chap. 1. Springer–Verlag, Berlin (1983).
2. Topsøe, H., and Rostrup-Nielsen, J. R., Scan. *J.* Metallurgy **8,** 168 (1979).
3. Rose, F., *Stahl Eisen* **95,** 1012 (1975).
4. Baker, R. T. K., and Harris, P. S., *in* "Chemistry and Physics of Carbon" Vol. 4 (P. L. Walker, Jr. and P. A. Thrower, Eds.), p. 83. Dekker, New York, 1978.
5. Rostrup-Nielsen, J. R., and Trimm, D. L., *J. Catal.* **48,** 155 (1977).
6. Williams, D. S., Möller, R., and Grabke, H. J., *High Temp. Sci.* **14,** 33 (1981).
7. Rostrup-Nielsen, J. R., *J. Catal.* **27,** 343 (1972).
8. Rostrup-Nielsen, J. R., and Christiansen, L. J., *in* "Proc. 6° Simposio Ibero-Americano de Catalise (Rio de Janeiro 1978), p. 1615. Instituto Brasileiro de Petróleo, 1981.
9. Perdereau, M., and Oudar, J., *Surf. Sci.* **20,** 80 (1970).
10. Alstrup, I., Rostrup-Nielsen, J. R., and Røen, S., *Appl. Catal.* **1,** 303 (1981).
11. Delescluse, P., and Masson, A., *Surf. Sci.* **100,** 423 (1980).
12. Sickafus, E. N., *Surf. Sci.* **19,** 181 (1970).
13. Rostrup-Nielsen, J. R., and Pedersen, K., *J. Catal.* **59,** 395 (1979).
14. Swift, H. E., Beuther, H., and Rennard Jr., R. J., *Ind. Eng. Chem. Prod. Res. Devlop.* **15,** 131 (1976).
15. Mol, A., *Hydrocarbon Process* **53,** 115 (1974).
16. Trimm, D. L., Holmen, A., and Lindvang, O., *J. Chem. Technol. Biotechnol.* **31,** 311 (1981).
17. Grabke, H. J., Möller, R., and Schnaas, A., *Werkst. Korros.* **30,** 794 (1979).
18. Rostrup-Nielsen, J. R., *J. Catal.* **31,** 173 (1973).
19. Bodrov, I. M., and Apel'baum, L. O., *Kinet. Katal.* **8,** 379 (1967).
20. Bohlbro, H., "An Investigation on the Kinetics of the Conversion of Carbon Monoxide with Water Vapour over Iron Oxide Based Catalysts." Gjellerup, Copenhagen, 1966.
21. Rostrup-Nielsen, J. R., *in* "Proc. Symp. on Science of Catalysis and its Application in Industry" Sindri 1979, FPDIL, p. XIII.
22. Kishi, K., and Roberts, M. W., *J. Chem. Soc. Faraday Trans. 1* **71,** 1715 (1975).
23. Kiskinova, M., and Goodman, D. W., *Surf. Sci.* **108,** 64 (1981).
24. Goodman, D. W., and Kiskinova, M., *Surf. Sci.* **105,** 265 (1981).
25. Erley, W., and Wagner, H., *J. Catal.* **53,** 287 (1978).
26. Münster, P., and Grabke, H. J., *J. Catal.* **72,** 279 (1981).
27. Kneale, B., and Ross, J. R. H., *J. Chem. Soc. Faraday Trans. I* **79,** 157 (1983).
28. Chahar, B. S., and Hightower, J. W., *J. Catal.*, in press.
29. Trimm, D. L., *Catal. Rev.—Sci. Eng.* **16,** 155 (1977).
30. Martin, G. A., *in* "Metal-Support and Metal-Additive Effects in Catalysis" (B. Imelik, C. Naccache, G. Courdurier, H. Praliaud, P. Meriaudeau, P. Gallezot, G. A. Martin, and J. C. Vedrine, Eds.), p. 315. Elsevier, Amsterdam, 1982.
31. Perdereau, J., and Rhead, G. E., *Surf. Sci.* **24,** 555 (1971).
32. Dowden, D. A. "Proceedings, 5th International Congress on Catalysis, (Florida 1972)," p. 621. North-Holland, Amsterdam, 1973.
33. Ponec, V., *Catal. Rev.—Sci. Eng.* **11,** 1 (1975).
34. Bartholomew, C. H., Agrawal, P. K., and Katzer, J. R., *Adv. Catal.* **31,** 135 (1983).
35. Bodrov, I. M., Apel'baum, L. O., and Temkin, M. I., *Kinet. Katal.* **9,** 1065 (1968).